

Bakker A., Cathie N., LaRoche R. (1994) Modeling of the Flow and Mixing in HEV Static Mixers. 8th European Conference on Mixing, September 21-23, 1994, Cambridge, U.K. IChemE Symposium Series No. 136, ISBN 0 85295 329 1, page 533-540.

ICHME SYMPOSIUM SERIES NO. 136

## MODELLING OF THE FLOW AND MIXING IN HEV STATIC MIXERS

*André Bakker*

Chemineer, Inc.

5870 Poe Avenue, Dayton, OH 45401-1123, USA

*Neil Cathie*

Chemineer Ltd., 7 Cranmer Road, West Meadows, Derby DE2 6XT, UK

*Richard LaRoche*

Cray Research, Inc., 655E Lone Oak Drive, Eagan, MN 55121, USA

The flow pattern and mixing characteristics of the High Efficiency Vortex (HEV) have been investigated by means of computational fluid dynamics simulations. Experiments showed that the HEV mixer generates a complex vortex system, consisting of a steady longitudinal vortex and transient hairpin vortices. The computer model correctly predicted the longitudinal vortex and a high turbulence intensity in the hairpin vortex region. The vortex system provides for efficient blending of gases or miscible liquids.

### 1. INTRODUCTION

Mixing is a common operation in the chemical process industries. Commonly used mixing devices are agitators for tanks and static mixers for pipe line mixing. The traditional helical mixing element (Kenics) is mainly used for in-line blending under laminar and transitional flow conditions. The High Efficiency Vortex (HEV™) is used for turbulent blending of gases or miscible liquids.

HEV mixers have been in use in the process industries for several years now, both for liquid-liquid and gas-gas mixing. The wide range of applications and scales in which the HEV mixer is used requires a technique to analyze custom applications on demand. The previous work on simulation of the flow in helical static mixers [1] indicates that computer simulation offers the right tool.

The flow pattern and mixing characteristics of HEV static mixers are analyzed through simulations with Fluent™ V4.21 for turbulent flow conditions. The computed flow patterns serve as a basis to calculate the mixing of two chemical species. The work reported here is limited to the mixing of two waterlike fluids, although simulations based on gas mixing have also been successfully completed.

### 2. SIMULATION

The model consisted of a 45° tube section with two vortex inducing tabs, see Figure 1. The tabs were set at an angle to the wall that was determined from previous research [2]. The length of the tube was  $L = 4.25 D$ , with  $D$  being the inner diameter. The first tab was placed at  $0.5 D$  down the tube, the second tab at  $1 D$  behind the first. This gave a little more than two and a half tube diameters of down stream mixing behind the last tab.

The grid was generated with Fluent PreBFC V4.01 and exported to Fluent V4.21 for the calculations and the post processing. Fluent was also used to scale the grid to the correct dimensions. The number of grid nodes was 100000. The outline of the geometry is shown in Figure 1.

A large liquid-liquid mixer was studied. The diameter was  $D = 2 \text{ m}$ . The length of the tube was  $8.5 \text{ m}$ . The fluid density was  $1000 \text{ kg.m}^{-3}$ . The viscosity was  $1 \text{ mPa.s}$ . The velocity in the tube was  $0.05 \text{ m.s}^{-1}$ , giving a Reynolds number of  $Re = 10^5$ . The diffusion coefficient was  $D = 1.5\text{E-}09 \text{ m}^2\text{s}^{-1}$ , for NaCl in water.

The calculations were performed using Fluent V4.21. The calculations were started with the  $k-\epsilon$

turbulence model. After 800 iterations the Reynolds Stress Model (RSM) was started, until the flow pattern was converged after about 1600 iterations. Then an additional 2000 iterations were made for the species, to make sure that the concentration field was fully converged. In all calculations the QUICK differencing scheme was used, rather than the power law scheme, to minimize numerical diffusion.

### 3. RESULTS OF FLOW PATTERN STUDIES

Figure 2 shows particle streaklines behind the second tab, which demonstrate the strong circulation flow in the wake of the tab. The vortex is attached to the wall of the tube and not to the tabs and lies parallel with the tab. The vortex then bends off to a longitudinal vortex with a center close to the tip of the tabs.

This is further clarified by Figures 3 to 5. Figure 3 shows the velocity vectors in a cross plane 0.5 D downstream of the second tab. The vectors point in the direction of the flow at the point where they originate. The length of the vectors is proportional to the velocity magnitude. Figure 3 clearly shows the vortex behind the tab. Figure 4 shows a similar flow pattern, but now 2.5 D downstream of the tab. The vortex still exists, but the swirl velocity is reduced by a factor of three. The top figure in Figure 5 shows the velocity magnitude in a longitudinal cross section of the tube, in the center of the tabs. Light areas denote large velocities and dark areas denote small velocities. The first tab directs the flow inward, accelerating the fluid. Behind the tabs there is a low velocity wake, which can also be seen from the velocity vector plot on the bottom of Figure 5. That figure shows that there is a small backflow region behind the tabs, which may induce some axial mixing, and smear out the residence time distribution.

Gretta [3] investigated the flow pattern as generated by the tabs using a combination of hot wire anemometry, hydrogen bubble visualization and dye visualization. Gretta discovered, see Figure 6, that the tabs not only generate a pair of counterrotating, longitudinal vortices but also shed so-called hairpin vortices. The smaller hairpin vortices move downstream with the larger longitudinal vortices.

The generation of these hairpin vortices is a transient process, and has also been experimentally observed by BHR Group [4]. Since the current model does not take time dependent effects into account, these vortices could not explicitly be modelled. However, the hairpin vortices do show up in the CFD results as regions with a large turbulence intensity. This is shown in Figures 7 and 8. Figure 7 displays the turbulent kinetic energy in a plane directly behind the first tab. Light areas denote regions with a large turbulence intensity. This plot shows that there is a region with a large turbulence intensity surrounding the vortex, where otherwise the hairpin vortex would be found. This is not surprising. The hairpin vortex is generated in the high shear region at the edge of the tab. In the steady state model used here, high shear increases the production of turbulent kinetic energy.

Figure 8 presents the turbulent kinetic energy in a plane through the center of the tabs. This plot also shows the high turbulence intensity generated at the edge of the tabs. In addition Figure 8 demonstrates that the turbulence intensity is higher behind the second tab than behind the first tab. This is an indication that the vortices reinforce each other.

### 4. RESULTS OF SPECIES MIXING STUDIES

To study the efficiency of the HEV mixer, the mixing of a tracer fluid was studied. The tracer fluid was injected at two positions, at the center of the tube and in a point located in front of a tab, see Figure 9. The total concentration of tracer fluid in the tube was 1.25 volume %.

Figure 10 shows the concentration field in a plane through the center of the tabs. Light areas denote regions with large concentrations of tracer fluid and dark areas denote low concentration regions. The injection in front of the tab is bent off when it hits the tab and is blended almost immediately in the turbulent wake of the tab. The injection in the center persists almost undisturbed until half way between the two tabs. There, the turbulence intensity generated by the vortex is large enough to blend the material in the center. These results indicate that is not just the longitudinal vortex which controls the blending, but that there is a significant contribution to the mixing by the hairpin vortex and random turbulence.

The Reynolds number for these simulations was  $10^5$ . When the Reynolds number is increased, e.g. to  $10^6$  or  $10^7$ , the distance within which the species mix  $l_{mix}$  will remain constant, or decrease slightly. This can be explained from turbulence theory. The distance from the inlet at which the species will be mixed  $l_{mix}$  is given by:

$$l_{mix} = v t_{mix} \quad (1)$$

Here  $v$  is the liquid velocity and  $t_{mix}$  is the mixing time. Penetration theory says that the time to mix two chemicals due to (turbulent) diffusion processes is inversely proportional to the (turbulent) diffusion constant:

$$t_{mix} \propto \frac{1}{D_t} \quad (2)$$

In other words, the mixing time will be cut in half when the diffusion constant increases by a factor of two. In turbulent flows mixing is dominated by the turbulent diffusion constant  $D_t$  (see Theory section). The turbulent diffusion constant is proportional to:

$$D_t \propto \frac{k^2}{\epsilon} \quad (3)$$

The energy dissipation rate is proportional to the multiple of the pressure drop  $\Delta p \propto v^2$  and the flow rate  $Q_t \propto v$ :

$$\epsilon \propto \Delta p Q_t \propto v^3 \quad (4)$$

At very low Reynolds numbers turbulent vortices will not exist (laminar flow). When the Reynolds number increases the vortices will start to grow, until at some point the flow is fully developed and the size of the vortices will be independent of the Reynolds number. Then the size of the largest turbulent eddies, the so-called Taylor macro scale  $L_t$ , will also be independent of the Reynolds number. The turbulent macro scale is given by:

$$L_t = \frac{k^{3/2}}{\epsilon} \quad (5)$$

This equation can be rewritten to show that:

$$k \propto (L_t \epsilon)^{2/3} \propto L_t^{2/3} v^2 \quad (6)$$

Combining the equations above results in:

$$l_{mix} \propto v \frac{1}{D_t} \propto v \frac{1}{v L_t^{4/3}} \propto \frac{1}{L_t^{4/3}} \quad (7)$$

The length within which the fluids will mix is thus independent of the fluid velocity but is solely determined by the Taylor macro scale of turbulence, which is of the order of half the diameter of the longitudinal vortex. When the vortices grow with increasing Reynolds number, the turbulent length scale will increase and the mixing length will decrease. Once the flow field is fully established, the vortices will not grow anymore due to the restrictions of the physical size of the tube, and both the Taylor scale and the mixing length will be independent of Reynolds number. The flow field plots showed that the vortices dominate the whole cross section of the tube, which is an indication that the flow field is fully developed at  $Re = 10^5$ . The mixing length will therefore show no, or only a small decrease with increasing Reynolds number. These results can therefore safely be used at higher Reynolds numbers.

These results confirm what was experimentally found by Alden Research Laboratory [5, 6]. The conclusion that the most advantageous injection point is not the center, but near the tabs, was also found experimentally by Fasano [2]. These simulations were performed for an added volume fraction of 1.25%. The fluids are homogeneously mixed when they leave the tube, meaning that in this situation smaller or larger additions would also be homogeneously mixed.

## 5. CONCLUSIONS

CFD calculations for the flow of water in a tube equipped with two arrays of HEV tabs were done. Since the geometry is symmetrical, only a 45° section of the tube had to be modelled. The symmetry condition, in combination with the steady state model, means that mass exchange from one vortex section to another is purely based on turbulence.

The CFD models correctly predict the formation of a pair of counterrotating, longitudinal vortices behind each tab. Transient hairpin vortices, observed by Gretta [3], show up as regions with a large turbulent kinetic energy density.

Directly behind the tabs, at the tube wall, there is a small region with backflow. This may introduce some axial mixing, and smear out the residence time distribution.

The turbulence intensity is larger in the vortex behind the second tab than in the vortex behind the first tab. This is an indication that the vortices reinforce each other.

The mixing process seems to consist of two steps. Fluid on the outside of the tube is blended when it gets entrained in the vortex system behind the first tab. Fluid injected in the center of the tube is blended near the second tab, where the turbulence intensity is at a maximum. It is advised that injection points are placed near the tabs. The least favorable injection point for small additions is the center of the tube.

All calculations were steady state. Time dependent effects like possible oscillations in the vortex positions and the shedding of hairpin vortices were not explicitly modelled. The additional blending due to these effects was therefore also not modelled.

## LITERATURE

- [1] Bakker A., Marshall E.M., 1992, Proceedings Fluent Users Conference, pp. 126-146 October 13-15, Burlington, Vermont
- [2] Fasano J.B., 1991, Presented Mixing XIII Conference, June 10-15, 1991, Banff, Canada
- [3] Gretta W.J., 1990, Masters Thesis, Lehigh University, Bethlehem, Pennsylvania
- [4] Video about HEV mixer, presented at BHR-FMP meeting 11-12 May 1993, Philadelphia (unpublished)
- [5] Alden Research Laboratory, Inc., 1992, report no. 194-92/C707 (unpublished)
- [6] Alden Research Laboratory, Inc., 1992, report no. 4501 (unpublished)

## NOTATION

|               |   |
|---------------|---|
| $c$           | Mass fraction of chemical species           |
| $D$           | Tube diameter                               |
| $D$           | Diffusion coefficient                       |
| $D_t$         | Turbulent diffusion coefficient             |
| $g_i$         | Gravitational acceleration in direction $i$ |
| $k$           | Turbulent kinetic energy density            |
| $l_{mix}$     | Length within which the fluids are mixed    |
| $L$           | Length of tube                              |
| $L_t$         | Taylor macro scale of turbulence            |
| $t_{mix}$     | Mixing time                                 |
| $p$           | Pressure                                    |
| $P_k$         | Production of $k$                           |
| $P_{ij}$      | Reynolds stress production term             |
| $Q_i$         | Volume flow rate                            |
| $Re$          | Reynolds number                             |
| $Sc_t$        | Turbulent Schmidt number                    |
| $u_i$         | Fluctuating velocity in direction $i$       |
| $U_i$         | Average velocity in direction $i$           |
| $v$           | Liquid velocity                             |
| $\delta_{ij}$ | Dirac delta function                        |
| $\epsilon$    | Turbulent energy dissipation rate density   |
| $\rho$        | Liquid density                              |
| $\tau_{ij}$   | Stress tensor                               |
| $\mu$         | Dynamic viscosity                           |
| $\mu_t$       | Turbulent dynamic viscosity                 |
| $\nu$         | Kinematic viscosity                         |
| $\nu_t$       | Turbulent kinematic viscosity               |
| $\sigma$      | Model constants                             |
| $\Phi_{ij}$   | Pressure-strain correlation term            |

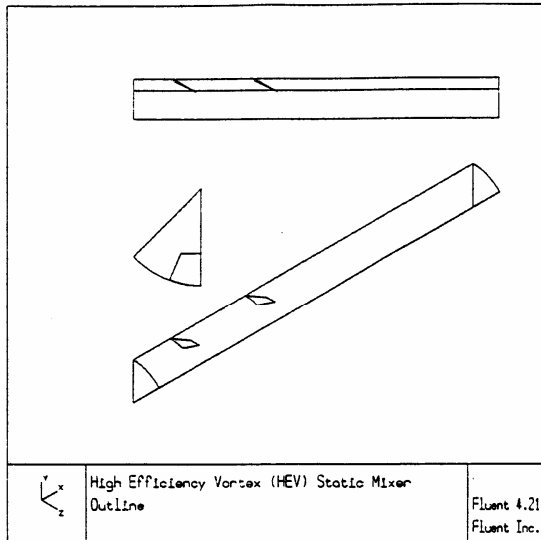


Figure 1 - Outline of tube with two HEV tabs

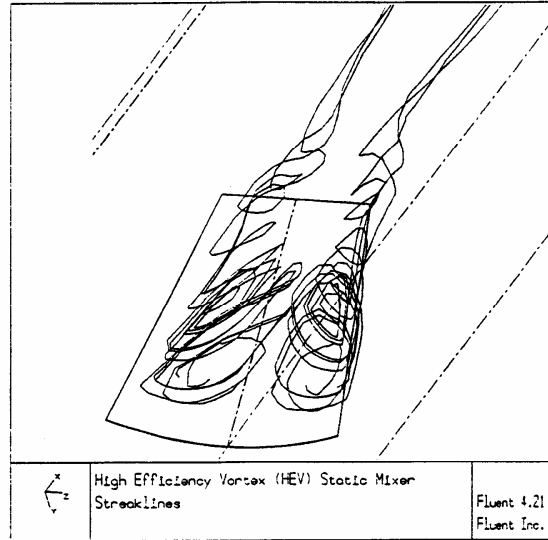


Figure 2 Trajectories of particles following the mean flow behind second tab (streaklines).

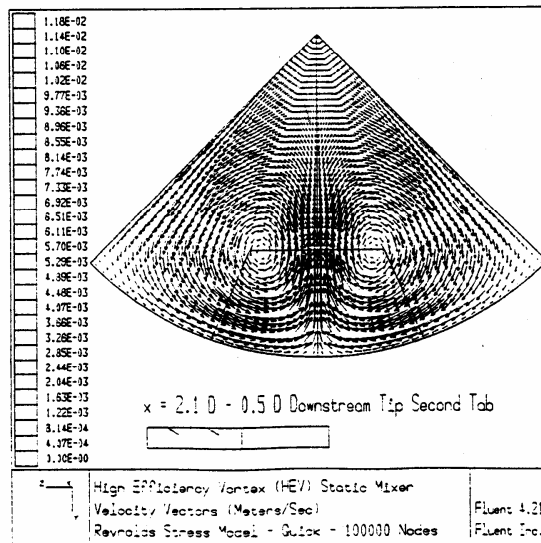


Figure 3 - Velocity vectors 0.5 D downstream of second tab.

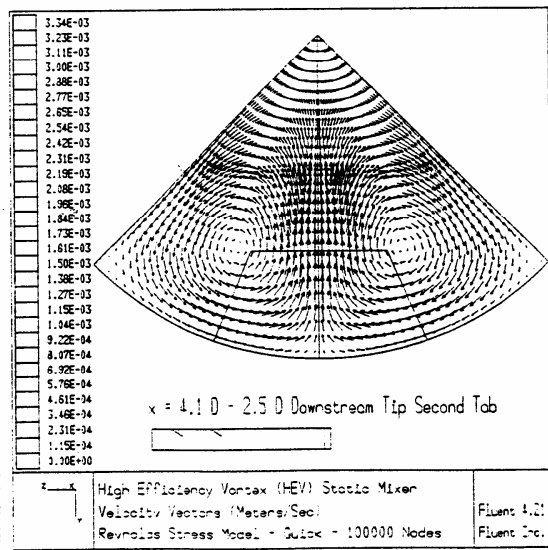


Figure 4 - Velocity vectors 2.5 D downstream of second tab.

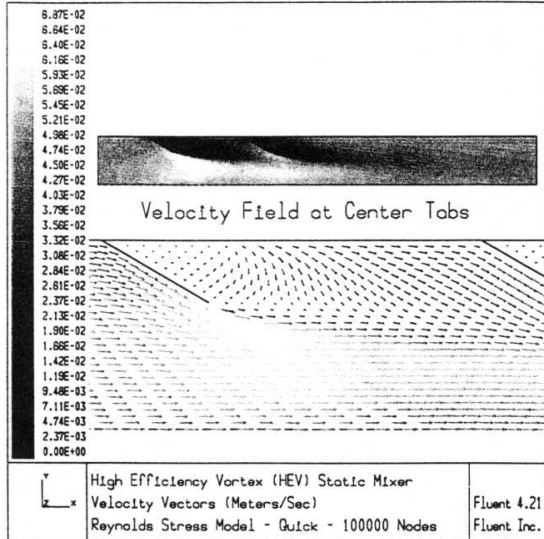


Figure 5 - Velocity magnitude and vectors in plane through center of tabs.

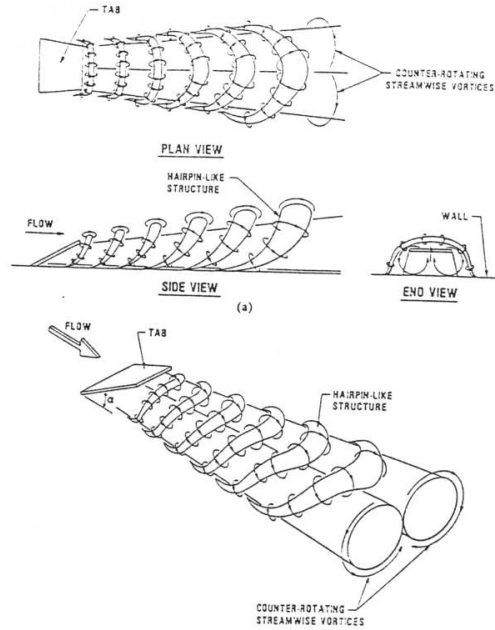


Figure 6 - Flow pattern according to Gretta

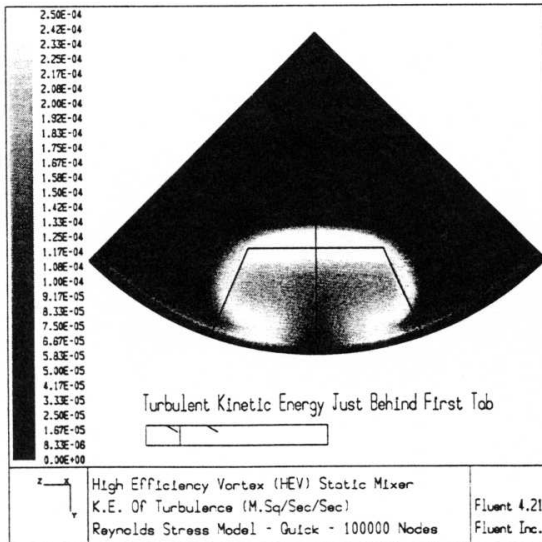


Figure 7 - Turbulent kinetic energy density just behind first tab.

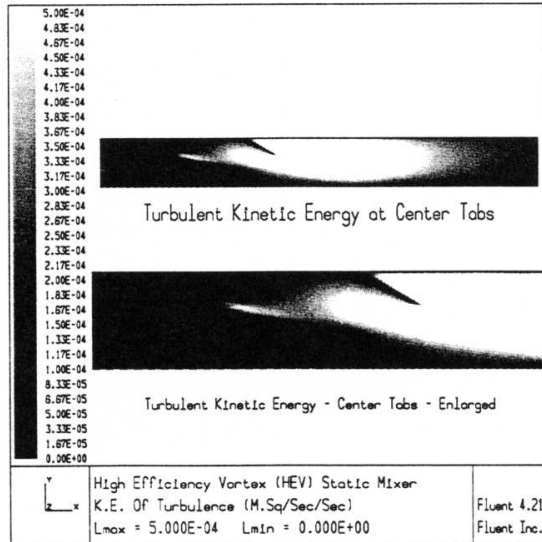


Figure 8 - Turbulent kinetic energy density in plane through tabs.

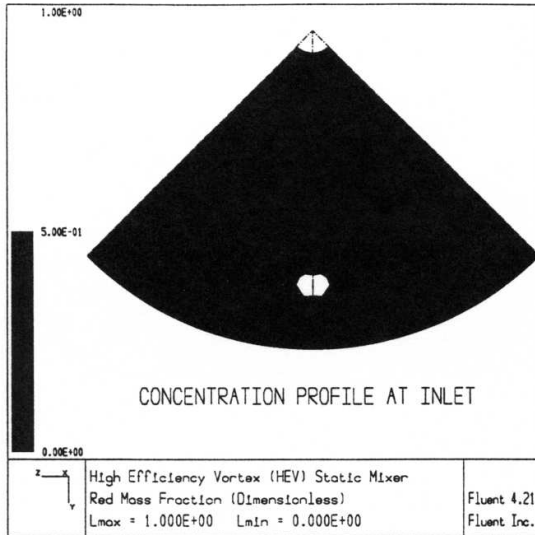


Figure 9 - Concentration of chemical species at inlet.

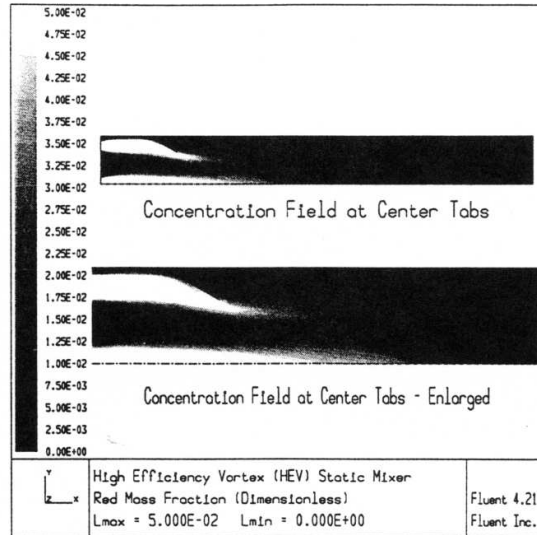


Figure 10 - Concentration of chemical species in plane through center tabs.